J Mater Sci: Mater Electron **(2025) 36:1083**

Influence of activated carbon concentration on the dielectric, conductivity and ımpedance properties of TPU composites

Sedat Kurnaz[1,*]

[1] *Central Research Laboratory, Kastamonu University, 37210 Kastamonu, Turkey*

Received: 20 February 2025
Accepted: 6 June 2025
Published online: 23 June 2025

ABSTRACT

This study examines the dielectric, electrical, and impedance properties of thermoplastic polyurethane (TPU) composites enhanced with activated carbon (AC) at concentrations ranging from 0 to 10% over a frequency range of 1 kHz to 10 MHz. The analysis includes capacitance, dielectric permittivity (ε', ε''), loss tangent ($tan\delta$), alternating current conductivity (σ_{ac}), electric modulus (M', M''), and impedance spectroscopy (Z, R, X, θ) to assess charge transport, polarization effects, and relaxation behavior. Results show that increasing AC content enhances interfacial polarization and charge mobility, improving dielectric performance and influencing conductivity mechanisms. Among the investigated composites, AC7 achieved the best balance of properties, with a dielectric constant of 54.47 at 10 kHz, an ac conductivity of 0.0169 μS/cm, and a loss tangent of 0.054 at the same frequency. This composition exhibited high charge storage capacity, stable impedance, and low dielectric losses, making it ideal for wearable technology, embedded capacitors, and supercapacitors. Its optimized electrical properties also support applications in flexible sensors and electronic packaging, where controlled impedance is crucial. This study highlights the importance of optimizing filler concentration to develop TPU-based composites with improved dielectric properties and minimal energy loss, making them suitable for high-frequency and energy-efficient applications.

1 Introduction

Thermoplastic polyurethane is widely used in flexible electronics and energy storage due to its excellent processability and chemical resistance [1]. However, its low dielectric constant and high dielectric loss limit its potential for high-performance electronic applications. To address this, conductive fillers are incorporated to enhance charge transport and dielectric properties [2]. The presence of AC facilitates interfacial polarization, improving charge storage efficiency and dielectric response through the Maxwell–Wagner-Sillars (MWS) effect below 1 MHz [3]. Achieving an optimal balance between high dielectric permittivity (high-κ) and low dielectric loss is essential for TPU composites to function effectively across a wide frequency spectrum.

High-κ materials play a crucial role in embedded capacitors and miniaturized electronic components,

Address correspondence to E-mail: sedatkurnaz@kastamonu.edu.tr

https://doi.org/10.1007/s10854-025-15154-7

where high capacitance values are required. According to the 1998 National Electronics Manufacturing Initiative (NEMI) roadmap, dielectric materials for embedded capacitors should have a dielectric constant of at least 100, low dielectric loss (< 0.05), and high breakdown voltage to ensure stable and reliable operation [4, 5]. However, improving the dielectric properties of TPU while maintaining its flexibility remains a challenge, particularly for applications in wearable electronics and high-frequency circuits.

Beyond conventional capacitor applications, TPU-conductive fillers composites are also gaining attention in flexible sensors and smart textiles, where stable dielectric behavior is critical [6, 7]. One of the main challenges in these applications is achieving high permittivity while minimizing energy losses. Increasing the amount of dielectric fillers (e.g., ceramics) raises permittivity but can also cause higher dielectric losses at certain frequencies. Conversely, conductive fillers like carbon nanotubes or graphene improve charge mobility, yet they may lower resistivity near the percolation threshold, leading to instability in electrical properties [8–12]. Addressing these challenges requires careful optimization of TPU-AC formulations to ensure stable dielectric properties across different operating conditions.

To improve the dielectric and impedance properties of TPU-AC composites, this study systematically investigates the effect of different AC loadings (0%, 3%, 5%, 7%, and 10%) on their dielectric constant, conductivity, and phase angle variations. The MWS effect plays a crucial role in charge accumulation at polymer-filler interfaces, improving permittivity at low frequencies but weakening at higher frequencies due to charge carrier relaxation [13]. By analyzing frequency-dependent dielectric behavior, this research provides a deeper understanding of TPU-AC composites' structure–property relationships and their potential electronic applications.

2 Materials and methods

2.1 Sample preparation method

TPU composites were prepared using the solvent-casting method, incorporating activated carbon (Tekkim Co. Ltd., Turkey) at different concentrations. The activated carbon used in this study has a surface area of ≥ 900 m^2/g, which helps improve dispersion in the polymer matrix. A total of 5 g of TPU (Hunan Solar Chemical Co. Ltd., China) was dissolved in a 40% N,N-Dimethylformamide (DMF)/60% Tetrahydrofuran (THF) solvent mixture (10 mL DMF / 15 mL THF) in glass beakers. Activated carbon was added at 0%, 1%, 3%, 5%, 7%, and 10% by weight, and the mixtures were stirred at room temperature for 140 min. An additional 4 mL DMF/6 mL THF was added to maintain homogeneity, and stirring continued for another 40 min. The final solutions were poured into glass petri dishes and dried in an oven at 50 °C for 17 h, forming flexible composite films. The prepared samples were labeled based on the activated carbon content as AC0 (0%), AC1 (1%), AC3 (3%), AC5 (5%), AC7 (7%), and AC10 (10%).

2.2 Characterization

The dielectric properties of the TPU-AC films were analyzed using a Wayne Kerr 6500B impedance analyzer in the 1 kHz to 10 MHz frequency range at room temperature. The complex dielectric permittivity (ε^*) describes the material's response to an alternating electric field and consists of and imaginary components. It is expressed as [5, 14]:

$$\varepsilon^* = \varepsilon' - i\varepsilon'' \tag{1}$$

The dielectric constant (ε') represents the material's charge storage capacity, which is influenced by dipolar and interfacial polarization, while the dielectric loss (ε'') quantifies energy dissipation, primarily caused by dielectric relaxation and charge carrier movement.

The dielectric loss tangent ($tan\delta$), also known as the dissipation factor, quantifies the ratio of energy lost to energy stored and is given by [15]:

$$\tan\delta = \frac{\varepsilon''}{\varepsilon'} \tag{2}$$

The alternating current conductivity (σ_{ac}) describes the frequency-dependent charge transport behavior and is determined using [16]:

$$\sigma_{ac} = \varepsilon_0 \omega \varepsilon'' = \omega \varepsilon_0 \varepsilon' \tan\delta \tag{3}$$

The angular frequency (ω) is defined as $\omega = 2\pi f$, where f is the applied signal frequency, and ε_0 represents the permittivity of free space, with a constant value of 8.854×10^{-12} F/m.

To reduce the impact of DC conductivity and achieve a clearer understanding of electrical relaxation

phenomena, the dielectric data, originally represented by the ε' and ε'' of ε^*, are transformed into the electric modulus (M^*), enabling a more effective analysis of charge carrier dynamics and interfacial polarization [17].

$$M^* = \frac{1}{\varepsilon^*} = M' + iM'' \tag{4}$$

where M' and M'' represent the real and imaginary components of the electric modulus, respectively. These components can be expressed in terms of complex dielectric permittivity as follows:

$$M' = \frac{\varepsilon'}{\varepsilon'^2 + \varepsilon''^2} \tag{5}$$

$$M'' = \frac{\varepsilon''}{\varepsilon'^2 + \varepsilon''^2} \tag{6}$$

The complex impedance (Z^*) is used to analyze dielectric relaxation and electrical resistance. It consists of real and imaginary components and is expressed as [18]:

$$Z^* = Z' - iZ'' \tag{7}$$

The real part of impedance (Z') corresponds to the resistive behavior of the material, indicating how charge carriers encounter opposition to their movement. The imaginary part (Z'') is associated with capacitive and inductive contributions, reflecting energy storage and dissipation within the material.

3 Results and discussion

Figure 1 illustrates the frequency-dependent dielectric behavior of composites containing different concentrations of AC (0–10%). Capacitance measurements reveal that composites exhibit higher capacitance at low frequencies, particularly for AC10, which reaches approximately 0.36 nF·cm^{-2} at 1 kHz. This enhancement is primarily due to interfacial polarization, where the conductive carbon network facilitates localized charge accumulation, improving the overall charge storage capacity. The inset graph highlights that composites with lower AC content show minimal capacitance changes, reinforcing that higher filler loading plays a key role in enhancing the dielectric response. As frequency increases beyond 1 MHz, capacitance decreases across all samples, as dipoles and charge carriers struggle to realign with the rapidly oscillating electric field. This behavior indicates that while high AC concentrations enhance low-frequency charge storage, their effectiveness diminishes in the high-frequency region, where dipolar relaxation mechanisms dominate (Table 1).

The ε' follows a similar trend, showing a notable increase for AC10, reaching 202 at 1 kHz. This increase is attributed to microcapacitive network formation within the polymer matrix, supported by the conductive nature of activated carbon. Higher filler concentrations amplify polarization effects, enhancing the ability of the composite to store electric energy. In contrast, samples with lower AC content exhibit relatively low ε' values, indicating weaker interfacial polarization effects. As frequency increases, all samples show a gradual decline in ε', with AC10 experiencing the steepest reduction. This drop is characteristic of dielectric relaxation, where charge carriers fail to keep up with fast-changing electric fields, leading to lower permittivity. The inset graph reveals that samples with lower filler concentrations maintain a relatively stable ε', indicating a more uniform dielectric response across the frequency range [19, 20].

The ε'' represents dielectric losses caused by polarization relaxation and charge mobility limitations. A distinct peak at ~ 110 kHz is observed for AC10, confirming the MWS interfacial polarization effect. This peak corresponds to the frequency range where accumulated charge carriers at the polymer-filler interface can no longer sustain polarization alignment, leading to significant dielectric losses [21]. In contrast, AC0 and AC1 show much lower ε'' values, indicating minimal interfacial polarization effects due to their lower conductive filler content. Beyond 110 kHz, ε'' sharply decreases, suggesting that at higher frequencies, charge carriers contribute less effectively to polarization mechanisms. These results confirm that while higher AC concentrations are beneficial at specific frequencies, excessive AC content can lead to significant dielectric losses, which may limit the material's suitability for high-frequency electronic applications. The broad relaxation peak observed in AC10 suggests a heterogeneous distribution of relaxation times, likely due to the complex interactions between dispersed filler particles and the polymer matrix.

The tanδ is a crucial parameter for evaluating dielectric energy dissipation relative to stored energy. AC10 exhibits a pronounced peak near 110 kHz, aligning with the ε'' peak, reinforcing the dominance

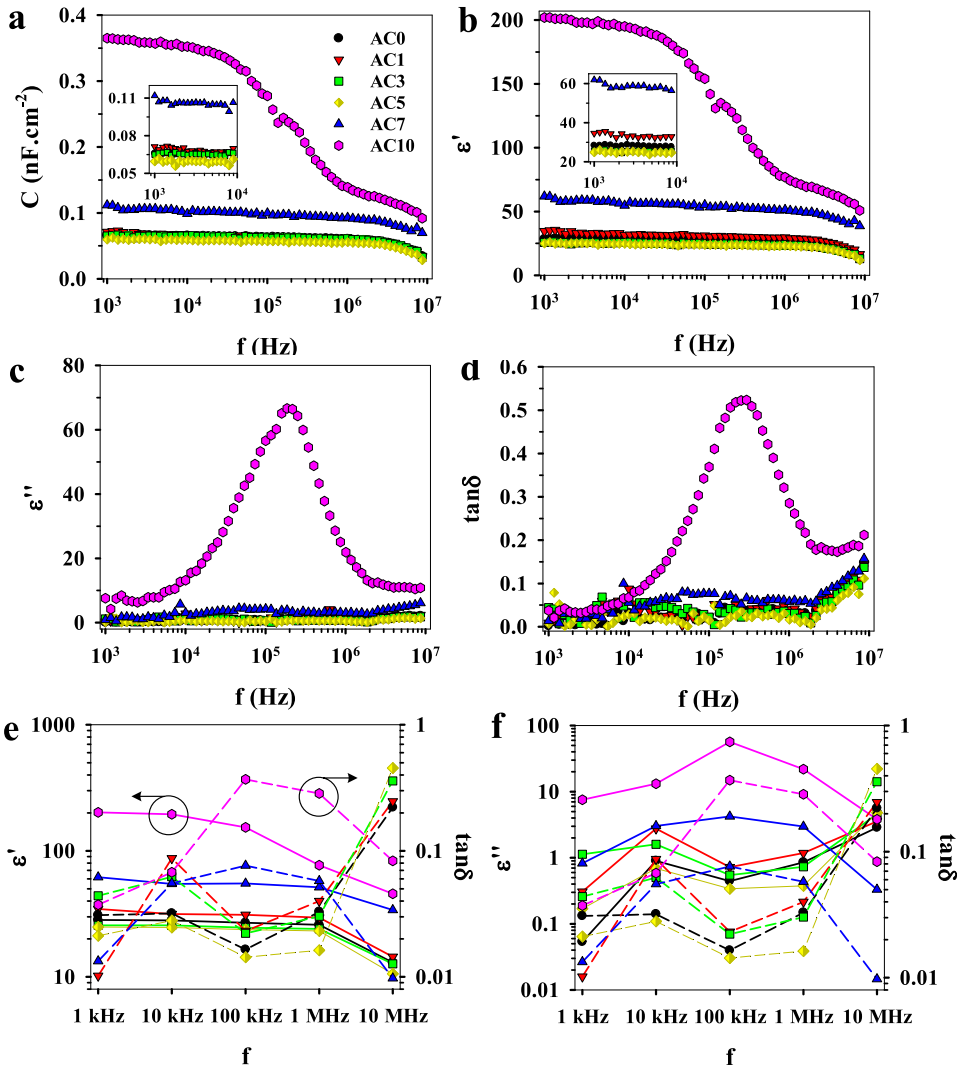

Fig. 1 Frequency-dependent dielectric properties. **a** *C*, **b** ε', **c** ε'', **d** tanδ, **e** comparison of ε' and tanδ, and **f** comparison of ε'' and tanδ

Table 1 Dielectric properties of TPU-AC composites at different frequencies

Sample	ε', ε'', *tanδ*				
	1 kHz	10 kHz	100 kHz	1 MHz	10 MHz
AC0	28.3, 0.05, 0.031	28.07, 0.90, 0.032	26.91, 0.443, 0.016	25.94, 0.85, 0.033	12.99, 2.87, 0.221
AC1	34.6, 0.31, 0.010	31.54, 2.76, 0.087	31.10, 0.721, 0.023	29.57, 1.18, 0.040	14.41, 3.56, 0.247
AC3	25.7, 1.13, 0.005	25.67, 1.6, 0.062	24.60, 0.55, 0.022	24.07, 0.73, 0.030	12.69, 4.56, 0.359
AC5	24.9, 0.17, 0.021	24.69, 0.69, 0.028	23.75, 0.34, 0.014	23.18, 0.38, 0.016	10.57, 4.8, 0.454
AC7	61.9, 0.83, 0.013	54.47, 3.03, 0.054	51.17, 4.22, 0.076	51.42, 2.97, 0.058	33.95, 0.33, 0.010
AC10	202,0 7.55, 0.037	194.98, 13.2, 0.068	153.53, 56.6, 0.369	76.89, 21.9, 0.285	45.69, 3.81, 0.083

of interfacial polarization at this frequency. This peak indicates substantial energy loss, caused by rapid polarization-depolarization cycles within the composite. Meanwhile, samples with lower AC content exhibit consistently low and stable *tanδ* values, suggesting a more efficient dielectric response with minimal energy dissipation. As frequency surpasses 1 MHz, *tanδ* decreases across all samples, reflecting the reduced influence of interfacial polarization on dielectric dissipation at higher frequencies. Notably,

AC5 and AC7 display a well-balanced *tanδ*, maintaining low dielectric losses while preserving adequate charge storage capacity.

The relationship between ε' and *tanδ* is evident across different frequency ranges (Fig. 1e). At low frequencies, AC10 exhibits the highest ε' (202 at 1 kHz), highlighting strong interfacial polarization driven by the MWS effect. This effect arises due to charge accumulation at polymer-filler interfaces, leading to the formation of localized capacitive structures. In contrast, samples with lower AC content display relatively stable but lower ε' values, indicating limited interfacial charge storage capacity.

Beyond 100 kHz, ε' decreases significantly for all samples, with AC10 showing the steepest decline. This drop reflects the reduced ability of dipoles and interfacial charges to realign with the high-frequency electric field. However, AC5 and AC7 maintain more stable ε' values, suggesting that an optimal filler concentration balances charge storage efficiency and frequency stability. Meanwhile, *tanδ* peaks at 110 kHz for AC10, indicating higher dielectric losses due to relaxation processes at this frequency. While higher filler loading enhances ε' at low frequencies, it also causes greater energy dissipation, making moderate AC concentrations more suitable for practical applications.

The ε'' provides insights into dielectric losses caused by charge carrier mobility constraints and polarization relaxation (Fig. 1f). AC10 exhibits a strong peak near 110 kHz, confirming the presence of MWS interfacial polarization and associated energy dissipation effects. This peak represents the frequency range where accumulated charge carriers lose their ability to sustain polarization alignment, leading to a sharp increase in dielectric loss. As the frequency increases further, ε″ declines across all samples, suggesting a transition from a polarization-dominated regime to a conduction-limited response. AC0 and AC1 maintain consistently low ε'' values across the entire frequency spectrum, reinforcing the minimal impact of interfacial polarization in these composites. Interestingly, AC5 and AC7 exhibit a more balanced distribution of ε'' and tanδ, indicating that these compositions are well-optimized for minimizing energy losses while maintaining sufficient dielectric performance.

The σ_{ac} strongly depends on both frequency and activated carbon concentration, exhibiting distinct charge transport mechanisms at different frequency ranges (Fig. 2). At low frequencies (1 kHz–10 kHz), the σ_{ac} remains relatively low across all samples, indicating that charge transport is primarily confined to localized carrier movement with limited conduction pathways. This behavior suggests that interfacial polarization dominates, and free charge carriers are not sufficiently activated for efficient conduction.

As the frequency increases beyond 10 kHz, a significant rise in σ_{ac} is observed, particularly for AC7 and AC10. This trend signifies a transition from interfacial polarization-driven transport to hopping conduction, where charge carriers gain enough energy to move between conductive sites. The sharp increase in σac aligns with percolation theory, which predicts that conductivity undergoes a drastic rise once a critical filler concentration is reached, leading to the formation of continuous conductive pathways within the polymer matrix [8, 9]. This behavior is further supported by the more gradual increase in σ_{ac} for moderate filler concentrations, suggesting the development of partial percolation networks. The inset graph highlights that lower filler concentrations exhibit minimal changes in conductivity with increasing frequency, reinforcing that these composites lack sufficient conductive networks to support free charge carrier transport. The presence of a critical percolation threshold is crucial

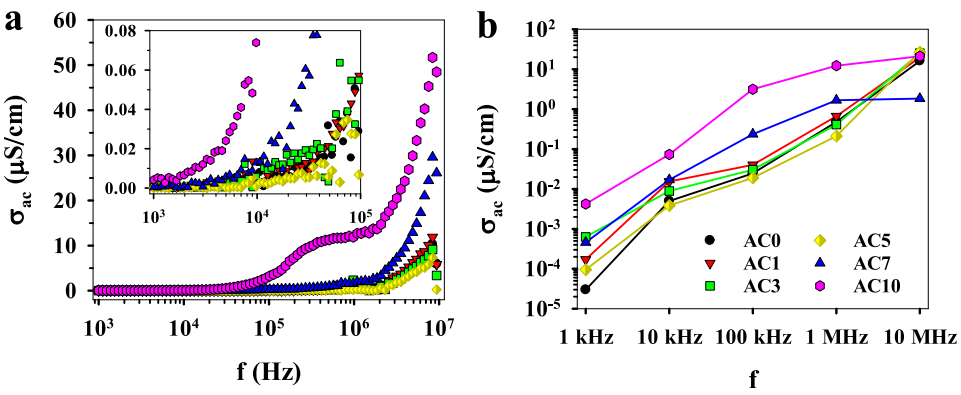

Fig. 2 Frequency-dependent ac conductivity. **a** σ_{ac}, **b** σ_{ac} on a logaritmic scale

for achieving high conductivity in polymer composites, as it dictates the transition from an insulating to a semi-conductive or conductive state [22–24].

Figure 2b, which presents the σ_{ac} on a logarithmic scale, further illustrates the increase in conductivity with both frequency and filler content (Table 2). The separation between the curves at higher frequencies confirms that enhanced charge carrier mobility in AC-rich composites enables more efficient conduction at elevated frequencies. However, excessive carbon loading may lead to agglomeration effects, potentially disrupting uniform charge transport and slightly reducing overall conductivity gains [21].

Figure 3 presents the electrical properties of polyurethane composites with varying AC concentrations over a frequency range of 1 kHz–10 MHz. The M' provides a measure of charge carrier confinement and energy storage efficiency (Fig. 3a). At low frequencies, M′ values remain minimal across all samples, suggesting highly mobile charge carriers with weak confinement. As frequency increases, M' gradually rises, with a more pronounced increase in higher AC content. This suggests that increased interactions between the polymer and conductive fillers restrict charge carrier movement. The noticeable increase in M' for the AC10 sample reflects strong MWS polarization effects, where charge accumulates at the interfaces between the filler and polymer, leading to higher resistance to electric flow. In contrast, AC5 and AC7 samples show a moderate and steady rise in M', indicating a balanced behavior suitable for high-frequency dielectric applications.

The M'' relates to energy loss and how the material responds to changing electric fields. In Fig. 3b, AC10 shows a clear peak between 100 kHz and 1 MHz, confirming that interfacial polarization and charge movement between sites are prominent. This peak indicates a shift where charge carriers move from localized areas to broader pathways, leading to increased energy loss. In contrast, samples with lower AC content do not exhibit such peaks, suggesting their response is mainly due to dipolar relaxation rather than interfacial effects. The broad peak for AC10 implies a wide range of relaxation times, common in conductive polymer composites due to uneven filler distribution. At frequencies above 1 MHz, M'' decreases for all samples, showing that interfacial polarization becomes less significant as charge carriers cannot keep up with the rapidly changing electric field [25].

Figure 4 presents the frequency-dependent impedance characteristics. In Fig. 4a, the Z decreases as frequency increases for all samples, a typical behavior in conductive polymer composites. At low frequencies (1 kHz–10 kHz), samples with low AC content (AC0, AC1) exhibit higher impedance, indicating limited charge transport. In contrast, the AC10 sample shows the lowest impedance, suggesting the formation of continuous conductive pathways. This trend aligns with percolation theory, where a critical filler concentration facilitates the transition from an insulating to a conductive state. [24, 26, 27].

Table 2 The σ_{ac} (μS/cm) at different frequencies

Sample	1 kHz	10 kHz	100 kHz	1 MHz	10 MHz
AC0	0.00003	0.0050	0.0247	0.480	16.0
AC1	0.00017	0.0154	0.0403	0.665	19.8
AC3	0.00063	0.0089	0.0305	0.410	25.3
AC5	0.00010	0.0039	0.0190	0.212	26.7
AC7	0.00046	0.0169	0.2360	1.670	1.84
AC10	0.00420	0.0736	3.1600	12.30	21.2

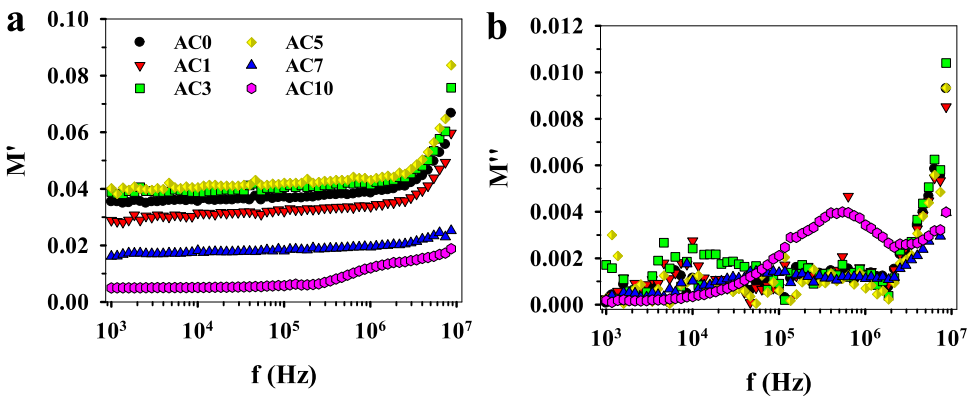

Fig. 3 Frequency-dependent electrical modulus. **a** M', **b** M''

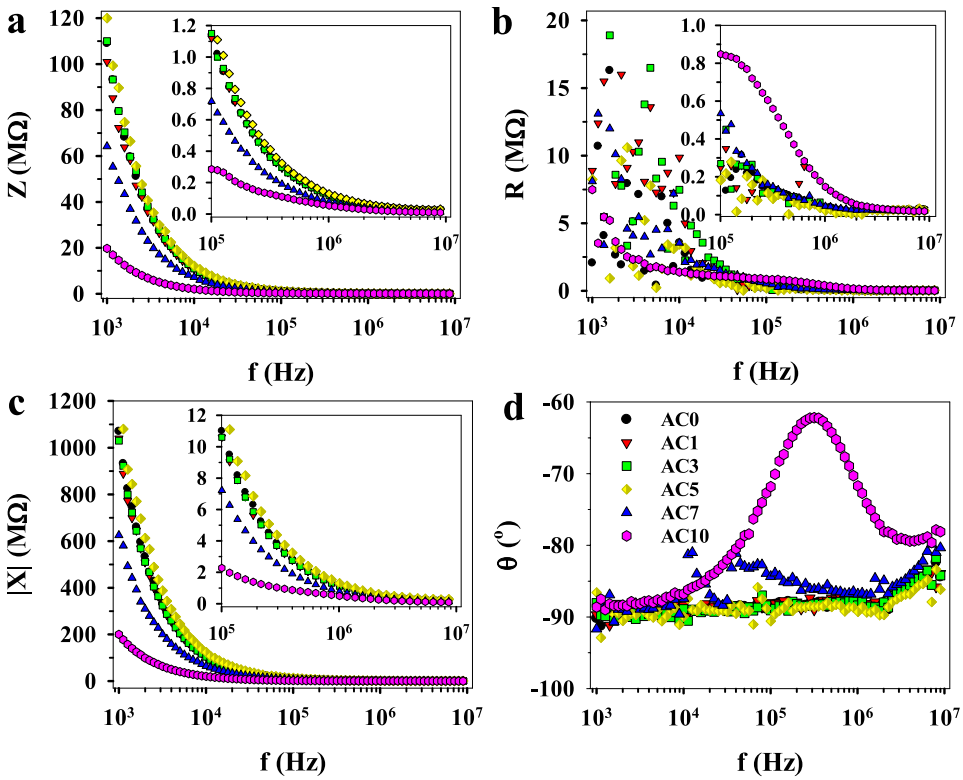

Fig. 4 Frequency-dependent impedance characteristics of composites with varying activated carbon concentrations: **a** Z, **b** R, **c** $|X|$, and **d** θ

The resistance (R) follows a similar pattern, decreasing with increasing frequency (Fig. 4b). The AC10 sample consistently exhibits the lowest resistance, confirming that higher filler content enhances charge transport. Samples with lower AC content maintain relatively high resistance across all frequencies, indicating poor formation of conductive networks. At frequencies above 1 MHz, resistance stabilizes, suggesting a shift from interfacial charge trapping to uniform charge transport mechanisms.

The reactance ($|X|$) provides insights into the capacitive and inductive contributions to impedance (Fig. 4c). At low frequencies, the AC10 sample shows the highest reactance, indicating strong capacitive energy storage due to interfacial polarization. As frequency increases, $|X|$ decreases sharply, suggesting that dipoles and interfacial charges cannot realign with the rapidly oscillating electric field. Beyond 1 MHz, all samples exhibit similar reactance values, implying that charge transport is now dominated by conduction rather than polarization effects.

The phase angle (θ) reveals the nature of the composites' electrical response (Fig. 4d). At low frequencies, θ is close to −90° for all samples, indicating dominant capacitive behavior. However, the AC10 sample displays a distinct peak near 100 kHz, reaching approximately -65°, marking the transition from capacitive to conductive behavior. This peak is associated with MWS polarization, where charge carriers accumulate at polymer-filler interfaces before transitioning to a conduction-dominated regime. At frequencies above 1 MHz, all samples return to around -90°, reflecting a predominantly dielectric response.

4 Conclusion

In this study, the dielectric, electrical, and impedance properties of polyurethane composites with varying activated carbon concentrations (0–10%) were investigated over a broad frequency range (1 kHz–10 MHz). The results demonstrated that filler concentration significantly influences charge transport, interfacial polarization, and dielectric relaxation mechanisms. A comprehensive analysis was conducted, covering capacitance, dielectric permittivity, loss tangent, AC conductivity, electric modulus, and impedance spectroscopy to evaluate the electrical behavior of TPU-AC composites.

The findings indicate that higher activated carbon content (AC10) enhances charge storage and interfacial polarization, but it also leads to greater

dielectric losses, particularly at mid-to-high frequencies. Conversely, low-filler-content samples (AC0, AC1) exhibited limited charge transport and weak polarization effects, making them less suitable for advanced electronic applications. Among all compositions, AC7 emerged as the most optimized material, demonstrating a balanced combination of high dielectric permittivity, moderate conductivity, and stable impedance behavior. Its ability to minimize dielectric losses while maintaining efficient charge storage makes it a strong candidate for high-frequency capacitors, supercapacitors, and embedded energy storage devices. Additionally, the impedance and electric modulus analysis revealed that AC7 maintains a well-regulated charge transport network, ensuring controlled relaxation dynamics and low-energy dissipation. The phase angle analysis further confirmed that AC7 exhibits an optimal transition between capacitive and conductive behavior, highlighting its potential for high-efficiency electronic and energy storage applications.

Overall, the study underscores the significance of precise filler concentration tuning to enhance the electrical performance of TPU composites. The results suggest that moderate activated carbon loading can effectively improve dielectric efficiency, reduce energy losses, and optimize charge transport, making these composites highly suitable for next-generation high-frequency, energy-efficient, and flexible electronic applications.

Author contributions

SK: Characterization, conceptualization, experiments, investigations, original draft writing, visulization, review and editing.

Funding

Open access funding provided by the Scientific and Technological Research Council of Türkiye (TÜBİTAK). This research was supported by Kastamonu University Scientific Research Projects Coordination Department under the Grant No. KUBAP-01/2022-28.

Data availability

The data that support the findings of this study are available upon reasonable request from the authors.

Declarations

Conflict of interest Author declares no conflict of interest regarding this paper.

References

1. D.P. Simunec, M. Breedon, F.R. Muhammad, Electrical capability of 3D printed unpoled polyvinylidene fluoride (PVDF)/thermoplastic polyurethane (TPU) sensors combined with carbon black and barium. Addit. Manuf. **73**, 103679 (2023)
2. J. Gómez, I. Recio, A. Navas, E. Villaro, Processing influence on dielectric, mechanical, and electrical properties of reduced graphene oxide–TPU nanocomposites. J. Appl. Polym. Sci. **136**(12), 47220 (2018)
3. G. Petrossian, N. Aliheidari, A. Ameli, Thermoplastic polyurethane/lead zirconate titanate/carbon nanotube composites with very high dielectric permittivity and low dielectric loss. J. Compos. Sci. **4**(3), 137 (2020)
4. S. Ogitani, S.A. Bidstrup-Allen, P.A. Kohl, Factors influencing the permittivity of polymer/ceramic composites for embedded capacitors. IEEE Trans. Adv. Packag. **23**, 313–322 (2000)

5. K.C. Kao, *Dielectric Phenomena in Solids* (Elsevier Academic Press, San Diego, 2004)
6. S. Liu, R. Duan, S. He, H. Liu, M. Huang, X. Liu, W. Liu, C. Zhu, Research progress on dielectric properties of PU and its application on capacitive sensors and OTFTs. React. Funct. Polym. **181**, 105420 (2022)
7. X. He, J. Zhou, L. Jin, X. Long, H. Wu, L. Xu, Y. Gong, W. Zhou, Improved dielectric properties of thermoplastic polyurethane elastomer filled with core–shell structured PDA@TiC particles. Materials **13**(15), 3341 (2020)
8. Z.M. Dang, J.K. Yuan, J.W. Zha, T. Zhou, S.T. Li, G.H. Hu, Fundamentals, processes, and applications of high-permittivity polymer-matrix composites. Prog. Mater. Sci. **57**, 660–723 (2012)
9. D. Wang, T. Zhou, J.-W. Zha, J. Zhao, C.-Y. Shi, Z.-M. Dang, Functionalized graphene–$BaTiO_3$/ferroelectric polymer nanodielectric composites with high permittivity, low dielectric loss, and low percolation threshold. J. Mater. Chem. A **1**, 6162–6168 (2013)
10. Z.M. Dang, M.S. Zheng, J.W. Zha, 1D/2D carbon nanomaterial-polymer dielectric composites with high permittivity for power energy storage applications. Small **12**, 1688–1701 (2016)
11. H. Lv, Y. Guo, Y. Zhao, H. Zhang, B. Zhang, G. Ji, Z.J. Xu, Achieving tunable electromagnetic absorber via graphene/carbon sphere composites. Carbon **110**, 130–137 (2016)
12. Y.Y. Huang, E.M. Terentjev, Tailoring the electrical properties of carbon nanotube-polymer composites. Adv. Funct. Mater. **20**, 4062–4068 (2010)
13. T. Allami, A. Alamiery, M.H. Nassir, A.H. Kadhum, Investigating physio-thermo-mechanical properties of polyurethane and thermoplastics nanocomposite in various applications. Polymers **13**(15), 2467 (2021)
14. V.F. Lvovich, *Impedance spectroscopy: applications to electrochemical and dielectric phenomena* (Wiley, New Jersey, 2012)
15. A. Sedky, N. Afify, A. Almohammedi, M.A. Sayed, A. Mossad Ali, A.M. Abd-Elnaiem, Structural, optical, and dielectric properties of M/SnO_2 (M = Al_2O_3, NiO, Mn_3O_4) nanocomposites. Ceram. Int. **50**, 3409–3421 (2024)
16. N. Chilaka, S. Ghosh, Dielectric studies of poly(ethylene glycol)-polyurethane/poly(methylmethacrylate)/montmorillonite composite. Electrochim. Acta **134**, 232–241 (2014)
17. Y. Nioua, B.M.G. Melo, P. Prezas, M.P.F. Graça, M.E. Achour, L.C. Costa, Analysis of the dielectric relaxation in reduced graphene oxide/epoxy composite materials using the modulus formalism. Eur. Phys. J. E **44**, 109 (2021)
18. R. Jose, L.A. Varghese, U.G. Panicker, Tailoring dielectric properties of natural rubber/millable polyurethane elastomer blends by filler embedding. Polym. Bull. **79**, 2041–2060 (2021)
19. J. Chen, P. Jiang, X. Huang, High dielectric constant (High-k) polymer composites. Encycl. Polym. Sci. Technol. **1**, 1–44 (2021)
20. X. Huang, B. Sun, Y. Zhu, S. Li, P. Jiang, High-k polymer nanocomposites with 1D filler for dielectric and energy storage applications. Prog. Mater. Sci. **100**, 187–225 (2018)
21. S. Siddabattuni, T.P. Schuman, Polymer-ceramic nanocomposite dielectrics for advanced energy storage. Polym. Compos. Energy Harvest. Convers. Storage **1161**, 165–190 (2014)
22. G. Shimoga, S.-Y. Kim, High-k polymer nanocomposite materials for technological applications. Appl. Sci. **10**, 4249 (2020)
23. J. Qiu, Q. Gu, Y. Sha, Y. Huang, M. Zhang, Z. Luo, Preparation and application of dielectric polymers with high permittivity and low energy loss: a mini review. J. Appl. Polym. Sci. **139**, e51882 (2022)
24. G. Teyssedre, C. Laurent, Charge transport modeling in insulating polymers: from molecular to macroscopic scale. IEEE Trans. Dielectr. Electr. Insul. **12**, 857–875 (2005)
25. J. Belattar, M.P.F. Graça, L.C. Costa, M.E. Achour, C. Brosseau, Electric modulus-based analysis of the dielectric relaxation in carbon black loaded polymer composites. J. Appl. Phys. **107**, 124111 (2010)
26. S.-H. Park, J. Hwang, G.-S. Park, J.-H. Ha, M. Zhang, D. Kim, D.-J. Yun, S. Lee, S.H. Lee, Modeling the electrical resistivity of polymer composites with segregated structures. Nat. Commun. **10**, 10514 (2019)
27. Z. Elimat, AC-impedance and dielectric properties of hybrid polymer composites. J. Compos. Mater. **49**, 3–15 (2013)